International Journal on Robotics, Automation and Sciences

Design and Development of an Arduino Based Automated Solar Grass Trimmer

Thangavel Bhuvaneswari*, Venugopal Chitra, Sarah Immanuel, Emerson Raja, Chua Wei Chern

***Abstract* – This paper focuses on the design of an Arduino-based Automated Solar Grass Trimmer with a primary emphasis on achieving high operational efficiency. A solar panel is utilized to automatically charge the battery when its level is low. A voltage level indicator circuit is incorporated to assess various battery voltage levels. The prototype integrates ultrasonic sensors for obstacle detection and inductive sensors for boundary detection. To ensure safe operation in the field, a perimeter signal generator circuit is constructed for boundary detection using inductive sensors. Ultrasonic sensors are employed for obstacle detection. The paper introduces an algorithm for detecting obstacles, boundaries, and other impediments in the path of the solar grass trimmer, illustrated through a comprehensive flowchart. Detailed discussions on the voltage level indicator circuit and boundary detection circuits are provided. The implemented algorithm, utilizing an Arduino microcontroller, is tested in the field, and the results are explained in the paper. Tabulated data from the prototype testing, specifically focusing on boundary detection and obstacle detection, demonstrate satisfactory performance.**

Keywords—Arduino Microcontroller, Perimeter Detection, Obstacle Detection, Solar, Grass Trimmer.

I. INTRODUCTION

The solar grass cutters have improved to the point where they can now self-dock and, if necessary, rain sensors, almost eliminating the need for human intervention. There have been several advancements in lawn mower technology throughout the years. However, as technology advances, it becomes essential to analyze the influence of robots on both the environment and humans. With a traditional gas-powered lawn mower, pollution is a serious problem. Another aspect that has to be eliminated is human effort. Such automatic lawn mower sales grown faster than regular lawn mowers. Some robotic mowers have improved the functionality within custom apps to alter settings or plan mowing time needs to be taken, it can also be manually operated by the user with a digital joystick, due to the rise of smart phones.

A microcontroller and sensor-based robotic lawn mower mechanism are used in this concept for the automated solar grass trimmer. When the battery on this solar-powered robotic lawnmower becomes low, the battery is charged by the sun. To avoid obstacles, an ultrasonic sensor is used. This design is intended

*Corresponding Author email: t.bhuvaneswari@mmu.edu.my, ORCID: 0000-0001-9022-2958
Thangavel Bhuvaneswari is with Faculty of Engineering and Technology, Multimedia University, Jalan Ayer Keroh Lama, 75450 Melaka, Malaysia phone: +6062523028, fax: +606 231 6552 (e-mail: t.bhuvaneswari@mmu.edu.my).
Venugopal chitra is from Department of Renewable Energy, Oregon Institute of Technology, Wilsonwille, OR, USA (email: chitra.venugopal@oit.edu)
Sarah Immanuel is *attached with Business and Information Systems*, *Torrens University, Australia* (email: sarah.immanuel@torrens.edu.au).
Emerson Raja, is with Faculty of Engineering and Technology, Jalan Ayer Keroh Lama, Multimedia University,75450 Melaka, Malaysia (email: emerson.raja@mmu.edu.my).
Chua Wei Chern is with Faculty of Engineering and Technology, Jalan Ayer Keroh Lama, Multimedia University,75450 Melaka, Malaysia(e-mail: busakthi2208@gmail.com)

International Journal on Robotics, Automation and Sciences (2024) 6,1:46-58
https://doi.org/10.33093/ijoras.2024.6.1.7
Manuscript received: 17 Nov 2023 | Revised: 29 Jan 2024 | Accepted: 19 Feb 2024 |
Published: : 30 Apr 2024

Published by MMU PRESS. URL: http://journals.mmupress.com/ijoras

to be a green alternative to the popular. The main issues addressed here are: The automated solar grass trimmer prototype requires the boundary to indicate the cutting area. A perimeter signal generator circuit is designed for boundary detection. Next, a solar panel is used to charge the batteries. LEDs are used to indicate the voltage level at different levels. Hence, a voltage level indicator circuit is designed to measure the voltage level of the 12V lead acid battery using LEDs. Lastly, to automate the solar grass trimmer, the moving path must be well-designed. A S shape pattern is used in the path design algorithm when it detects the boundary using the perimeter generator signal. When an obstacle is detected, the prototype turns left, moves forward a short distance, then turns right, moves forward.

F. Ocholi et al. introduced a solar-assisted lawn mower featuring an Arduino microcontroller-based control system [1]. The incorporation of a mobile application enhances functionality, allowing users to interact with the mower remotely. The rigorous simulation analysis of assembly stress and stability during turns provides valuable insights into the real-world performance of this design. Vitthal K. Khemnar et al. designed a solar-powered grass cutter incorporating a direct current (D.C.) motor, rechargeable battery, solar panel, shearing action blade, and an IoT-based control system [2]. The automated switching functions accessible through smart devices optimize energy usage and demonstrate superior efficiency compared to conventional cutters across various grass types. Ajay D. Shah et al. proposed an automatic grass cutter operating on solar energy, with provision for mains power charging during adverse weather conditions [3]. The user-driven input for specifying cutting area dimensions facilitates precise and efficient grass cutting, ensuring continuous operation for up to 2 hours on a fully charged battery.

Sherly Stalin et al. introduced an innovative grass cutter integrated with an Arduino microcontroller and IoT technology [4]. The BLYNK mobile application tracks the mower's movement through a Bluetooth module, while a Node MCU manages the DC motor's speed and direction. This integration enhances user control and monitoring capabilities. Snehal Popat Jagdale et al. proposed an Android smartphone-controlled grass cutter robot, utilizing a voltage regulator to convert battery supply for microcontroller operation [5]. Bluetooth technology facilitates seamless communication between the smartphone and the grass cutter, granting users full control over its movement. N. Nagarajan and colleagues introduced a grass cutting system with a helix-shaped blade design, demonstrating high efficiency, cost-effectiveness, and user-friendliness. The spiral blade mower's successful fabrication and testing validate its potential to revolutionize lawn care and maintenance [6].

Ramos, D proposed an autonomous lawn mower equipped with an array of sensors for object detection and avoidance [7]. Notably, this design eliminates the need for perimeter wires to constrain the robot within the lawn, enhancing its adaptability and user-friendliness. Shyam M. Ramnani et al. proposed an unmanned automated lawn mower with features for grass cutting and collection [8]. This cost-effective design incorporates a recyclable grass collector, emphasizing environmental sustainability in lawn maintenance.

Olawale Olaniyi Emmanuel AJIBOLA proposed an automated lawn mower with a dual charging system, utilizing both solar energy and AC supply [9]. Equipped with proximity sensors for object detection, this environmentally friendly design offers semi-autonomous and full-autonomous operation options, minimizing running costs.

The design and fabrication of a low-cost Dual Axis Solar Tracker (DAST) is proposed by Thangavel Bhuvaneswari et. al. [10]. The low-cost mechanical structure has been fabricated and stress analysis has been performed. A mechanical structure developed in Ref [10] is used for experimental studies in Ref [11 and 12]. The microcontroller with 4 LDR sensors to identify the maximum intensity of sunlight. Hence LDR sensors act as input to the microcontroller. The rotation of the motor (counter clockwise /clockwise) is performed by using a stepper motor with a pulley and belt, while the elevation(up/down) is controlled by a linear actuator. Then the sensors will compare the other two values north and south and the motor will move based on the largest value. After the north west movement and the cycle is going to be repeated. Dual axis solar tracker with Arduino microcontroller has been successfully designed and tested successfully at low cost. Dual axis tracking is verified along with MPPT controllers. It is observed that tracking is better than fixed panel, and it is much better with MPPT controller.

Solar panel tracking systems play a vital role in the efficient operation of solar power systems. In Ref [13] a survey on intelligent controllers based on solar panel tracking systems to identify various issues has a potential for further research. After summarizing the existing work, a proposal is made for the application of neuro-fuzzy controller for solar panel tracking systems for further improving their performance. Gitte Rajshree Rajeshwar and colleagues introduced an innovative solar-powered, fully automated grass-cutting vehicle equipped with obstacle avoidance capabilities [14]. This system relies on 12V batteries to drive both the vehicle's movement motors and the grass cutter. These motors, along with the grass cutter, are seamlessly integrated with an Arduino family microcontroller, which orchestrates their coordinated operation [15]. When an object is detected by the microcontroller, the robot pauses until the obstacle is cleared, at which point it resumes forward movement with the grass cutter in operation.

In ref [16], the envisioned Automatic Solar Grass Cutter machine designed to harness solar energy for battery charging, while employing a sonar sensor to identify and circumvent extraneous objects in the lawn

during its operation is proposed by Ahsan Niazi, et. al. This robotic system is comprised of an Arduino Mega 2560 microcontroller and cutting blades driven by a geared DC motor, with the battery serving as the power source for the motors [17]. Additionally, the battery can be recharged through a solar panel. Sonar sensors are deployed for obstacle detection along the robot's path [18].

The proposed methodology is clearly discussed in the following section II with several subsections; Perimeter signal generator circuit, LM324N Voltage Level Indicator Circuit, Reading the analog value from the perimeter wire and Arduino IDE programming. The proposed algorithm in the form of its flow chart, Testing the algorithm for boundary detection and obstacle detection are clearly analyzed in Section III, Results and Discussion. The conclusion of this paper is found in the last section IV.

II. METHODOLOGY

The block diagram of an automated solar grass trimmer is shown in Figure 1. The circuit and the Arduino mega 2560 micro-controller are to be powered up by a rechargeable 12V lead acid battery. When the battery is low, the solar panel is activated to charge the 12V battery, since the voltage from the solar panel is higher than the battery, a DC-DC buck converter is used to step down the voltage. Two types of sensors are used; an inductive sensor for boundary detection and an ultrasonic sensor for obstacle detection. The PWM motor speed control is used for grass trimming high speed motor, so that the motor speed can be manipulated. In addition to driving the prototype, the L298N motor driver is used to control the two low-rpm DC motors (left and right), lower rpm provides higher torque.

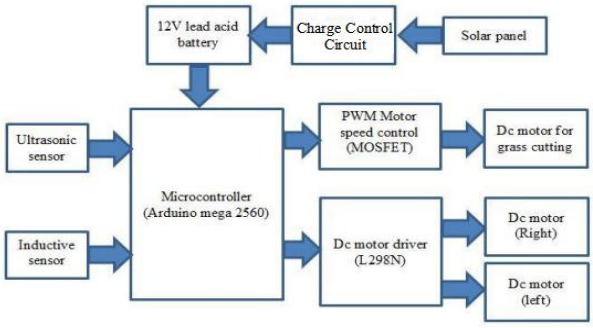

FIGURE 1. Block diagram of automated solar grass trimmer.

A. Perimeter Signal Generator Circuit

The automated solar grass trimmer requires the boundary to indicate the cutting area. NE555 timer is used to detect the boundary. NE555 in astable mode is used as an oscillator. The oscillation frequency and the duty cycle can be adjusted using two resistors and a capacitor. The schematic for astable mode is shown in Figure 2(a). The capacitors are continually charged through two resistors when a voltage is applied to the circuit, resulting in pulses. By short-circuiting the pins 2 and 6 will make the circuit to be restarted indefinitely. The capacitor in the circuit discharges completely if the output trigger pulse is high. Longer time delays are achieved by utilizing higher resistor and capacitor values. The NE555 generates a (rough) square wave that may travel the whole length of the perimeter wire. The formula to calculate the frequency of the output square wave for the 555 timer is shown in equation1:

$$Frequency, F = \frac{1.44}{(Ra + 2Rb) * C} \qquad (1)$$

The frequency generated will be 33.570 KHz to 45.867 KHz (square wave), which is a frequency that should not interfere with any adjacent equipment.

Let R_A = 3.3 k**Ω**, R_B= 12 k**Ω** + 5 k**Ω** potentiometer, and C = 1.2 nF (1nF + 200pF in parallel).

The purpose of potentiometer is to modify the square wave output frequency to match the LC Tank circuit's resonance frequency. The logically minimum and maximum output frequency values (F_L and F_H) are calculated as 32.172KHz and 43.956KHz. Since the 5K**Ω** potentiometer will never get to exactly 0 or 5k**Ω**, the output frequency range will vary between 32.172 KHz to 43.956 KHz. The schematic of the complete circuit is shown in Figure 2(b).

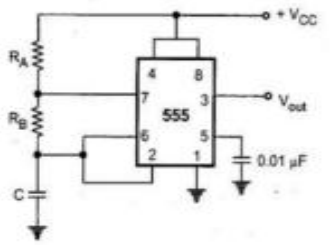

FIGURE 2(A). 555timer in a stable mode.

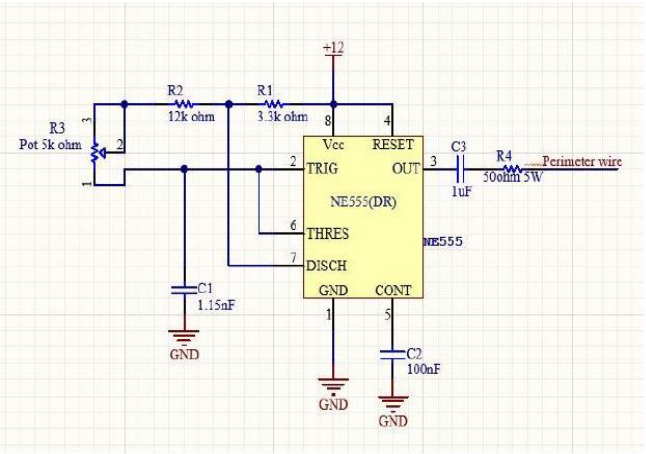

FIGURE 2(B). Perimeter signal generator circuit.

The circuit is powered by a 12V power supply, a square wave with a frequency range of 32.29 KHz -

39.12 KHz and an amplitude of 17V (with spike of roughly 5V and wave with 12V peak to peak) can be observed from the Oscillator screen as shown in Figure 3(a) and 3(b). By adjusting the R_3 potentiometer, the frequency can be manipulated between the actual frequency.

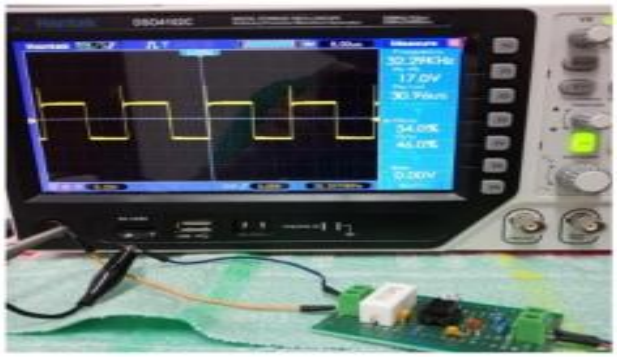

FIGURE 3(A). Output waveforms at minimum frequency.

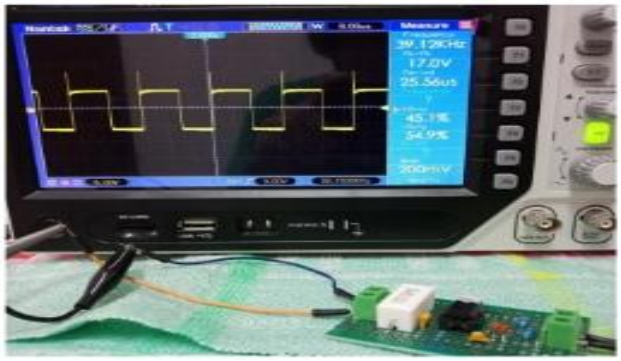

FIGURE 3(B). Output waveforms at maximum frequency.

After the perimeter signal generating circuit, an LC circuit is used to detect the signal flow through the wire using the formula as shown in equation 2.

$$Resonance\ Frequency, f = \frac{1}{2\pi\sqrt{L} * C} \qquad (2)$$

Where L is the coil's inductance in H (Henry) and C is the capacitor's capacitance in (Farads). The tank circuit should have a resonance frequency in this range for the sensor to detect the 33.570 KHz to 45.867 KHz signal that flows into the wire. By using the equation (2), L = 1mH and C = 22nF, the calculated resonance frequency is 33.932 KHz. When the inductor is around 5cm from the perimeter wire that generating signal, the amplitude of the signal sensed by the tank circuit will be detect a very low voltage of about 100mV as shown in Figure 4.

FIGURE 4. The inductor when close to the perimeter wire (no amplification).

That means this signal can be utilized to detect the boundary, since the voltage is really low, it needs to go through an amplification process. A weak electric signal can be amplified using an operational amplifier. LM324N for amplification with a gain of 100, and arranged in a non-inverting configuration with two stage amplification to make sure the output obtained a readable analog signal at a greater distance than 5cm in the output of the sensor using the formula as shown in equation (3).

$$Av = 1 + \frac{R2}{R1} \qquad (3)$$

Resistors R_1= 10k**Ω** and R_2 = 1M**Ω** are used to get a gain of 100, which is within the required range. It is preferable to have more than one sensor put on the prototype in order for it to detect the boundary wire in different orientations. The greater the number of sensors on the prototype, the better it will detect the boundary wire. Hence, three sensors are installed on the grass trimmer (left, right and front) below the prototype. Since the LM324N is a quad-op amp, this means it consists of 4 separate amplifiers. For each inductor sensor it needs to go through two amplification stage. For this design, the grass trimmer is installed with three inductors as sensor, therefore two LM324N or 6 amplifiers are to be used. The LM324N amplification schematic and its the completed circuit are shown in Figure 5(a, b and c) and 5(d) respectively.

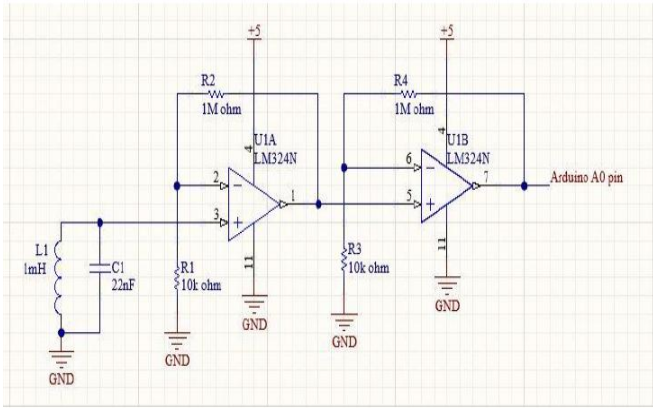

FIGURE 5(A). The lm324n amplification schematic.

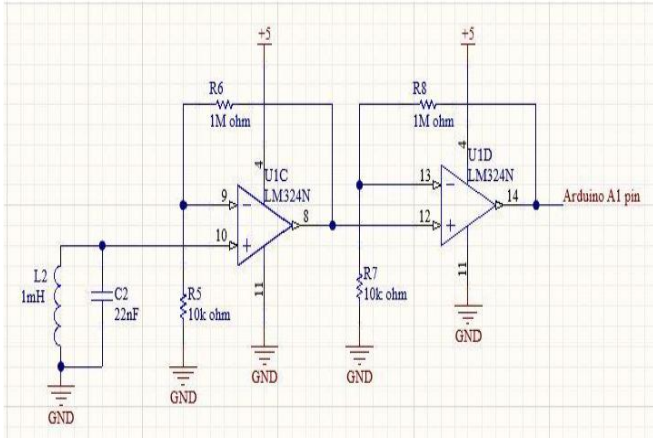

FIGURE 5(B). The lm324n amplification schematic.

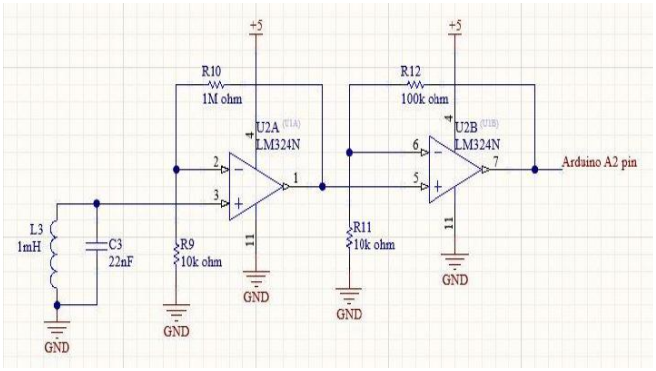

FIGURE 5(C). The lm324n amplification schematic.

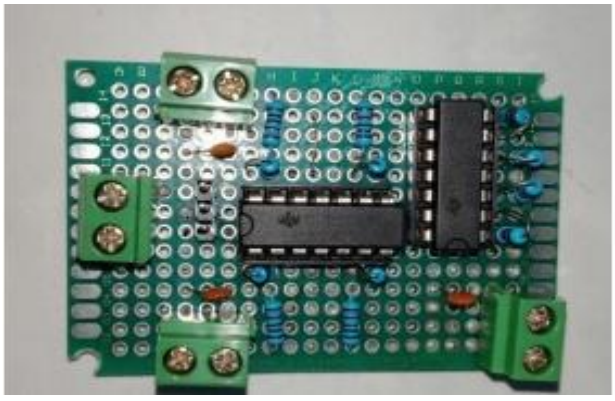

FIGURE 5(D). The complete lm324n amplification circuit.

The inductor is connected to the screw terminals on the circuit. The three output of the amplifier are connected to the analog input ports of the microcontroller. Arduino mega 2560 has 15 analog pins and each output is connected to A_0, A_1 and A_2 accordingly. The analog signal (detect wave) from the sensor board will range between 0V and 5V, it will depend on the distance between the inductor and the perimeter wire, since the LM324 chip is supplied by a 5V power source. The amplitude of the output of the sensor increases as the inductor gets closer to the perimeter wire. When the inductor sensor stays closer to the perimeter wire (about 5cm), the peak to peak voltage from the screen of the oscilloscope shows 1.20V peak to peak. When inductor gets even closer to the perimeter, the peak to peak value increase to 2V peak to peak and voltage clipped-off and saturated because it reached the maximum supply voltage. The reading from the oscilloscope is quite low because of the voltage drop at the supply voltage. The output waveform is shown in Figure 6(a) and 6(b) respectively.

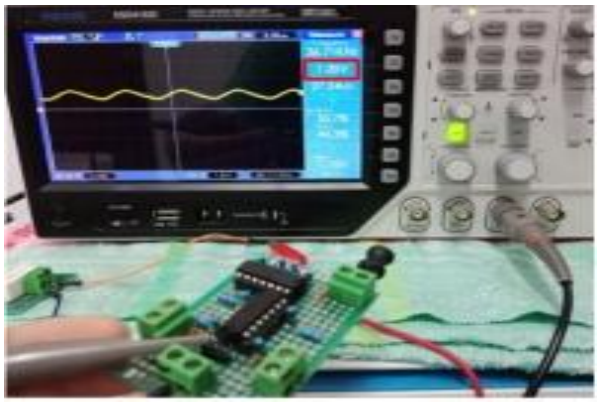

FIGURE 6(A). The inductor closer to the perimeter wire (after amplification).

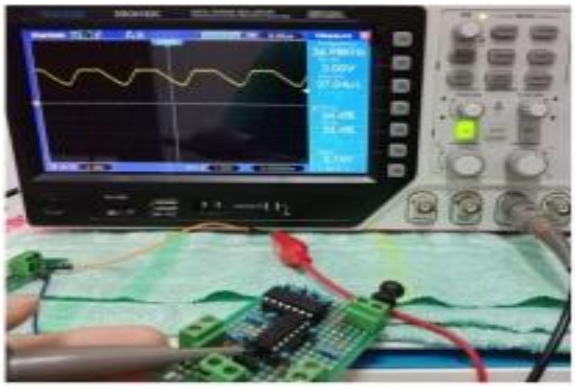

FIGURE 6(B). The inductor even closer to the perimeter wire (after amplification).

B. Reading The Analog Value from the Perimeter Wire

The Arduino code for reading the value from the sensor is quite simple. The AnalogRead command of

the Arduino may be used since the sensor board's output is analog signals ranging from 0V to 5V (0 to 1024). By simply connecting the sensor's amplifier circuit output pins to analog input pins and reading the appropriate pin by using the Arduino AnalogRead. Then, display the value in the serial monitor, should able to observe the RAW value of the analog pin ranging from 0 to 1024 as inductor sensor get closer to the perimeter wire. For Instance, by considering the inductor sensor at the front of the prototype which is boundary sensor two, when the perimeter wire away from the inductor, the analog value read from the sensor for this case was 13 as indicated in the serial monitor. Thus, no boundary is detected as shown in Figure 7(a) and the serial monitor output is shown in Figure 7(b).

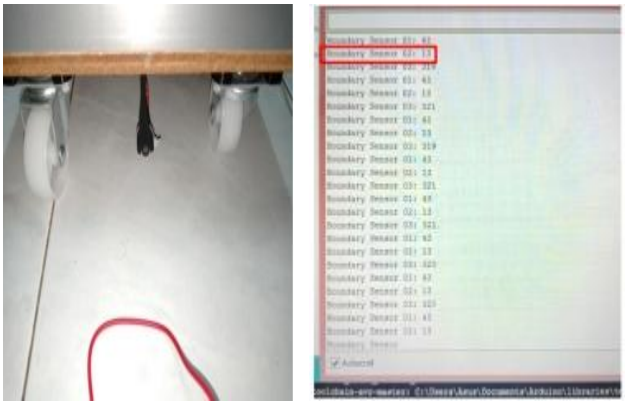

(a) (b)

FIGURE 7(A).The front inductor below of the prototype is away from perimeter wire; FIGURE 7(B). The analog value read from the serial monitor (away).

When the perimeter wire gets closer to the inductor, the reading from the analog pin value increase to 766, this mean the boundary was detected by the sensor. The closer the distance between the perimeter wire and the inductor, the higher the analog value reading obtained by the microcontroller as shown in Figure 7(c) and 7(d) respectively.

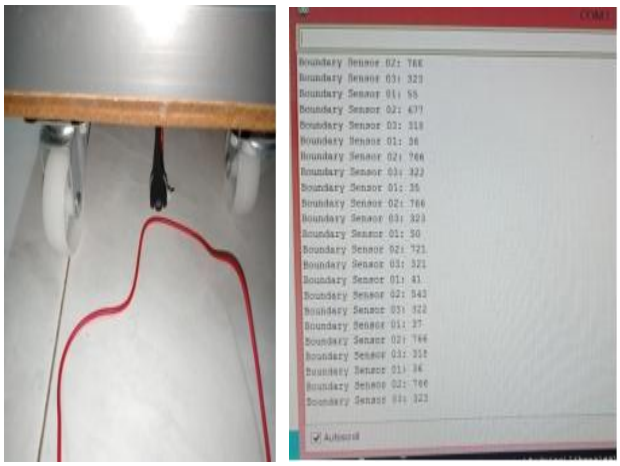

(c) (d)

FIGURE 7(C). The front inductor below the prototype close to the inductor; figure 7(d). The analog value read from the inductor (closer).

C. LM324N Voltage Level Indicator Circuit

The circuit uses the LM324N operational amplifier to measure the voltage level of the 12V lead acid battery, Eight LEDs are used to indicate the voltage level at different levels. So, from the LED display, the battery capacity can be determined. For 8 LEDs and 8 operational amplifiers 2 LM324N ICs are required. In the circuit, two potentiometer 50K**Ω** and 200K**Ω** and eight 1K**Ω** resistors are used to build the voltage divider and the operational amplifier is inverting amplifier, input signal is at the negative terminal of the operational amplifier. When negative terminal's voltage is greater than the positive terminal's voltage, the output is grounded and LED will light up.

The 50K**Ω** pot is used to tune the voltage level, since the voltage measured is less than the supply voltage. For example, the input voltage is 15V and the voltage measured is within the range of 12V - 13V, then tune the 50k pot until the voltage drop of the 50K**Ω** pot is 2V, from the voltage divider rule it is known that the voltage level after the 50K**Ω** pot is left 13V.

The 200k pot is used to tune the gap between the voltage to light up each LED. For example, for 8 LEDS to light up in sequence in 1V (12V – 13V), each increment of 0.125V will cause one led to light up. To obtain such condition, tune the 200k pot until it reaches the voltage drop of 12V, then the voltage drop for each 1K**Ω** resistor is 0.125V. Schematic of the one of the voltage level indicator circuit is shown in Figure 8(a) and the complete schematic circuit is shown in Figure 8(b).

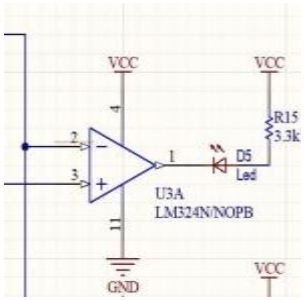

FIGURE 8(A). One of the op-amp voltage level indicator.

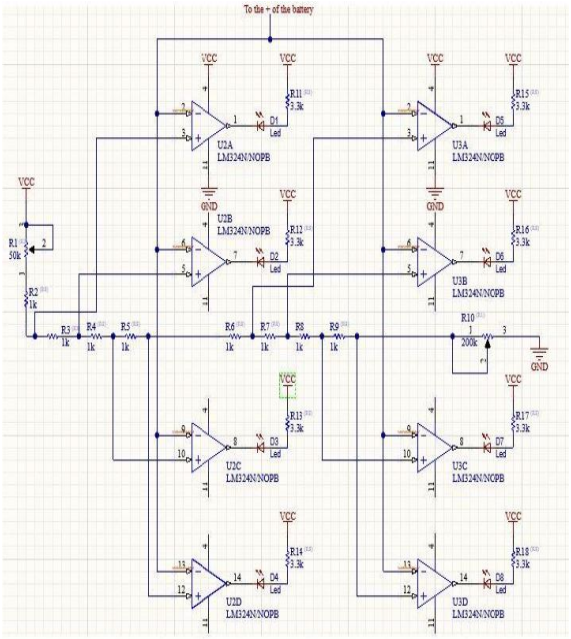

FIGURE 8(B). Complete schematic of the voltage level indicator.

Assume the voltage of the 12V lead acid battery's lowest voltage is 12V and highest voltage is 13V, i.e. 13V minus 12V, we left only 1V to indicate the lowest point and the highest point voltage of the battery, 1V will be divided by 8 and we get 0.125V. This means for every increment of 0.125V, one LED will light up from a red LED to blue LED. The voltage measure from the multi-meter is 12.6V while 5 LEDs light up. This shows the design is correct, because 12 + (5 x 0.125V) = 12.625V. The Complete Voltage Level Indicator circuit is shown in Figure 8(c). The complete circuit connection of the Arduino board with sensors and motors is shown in Figure-8(d).

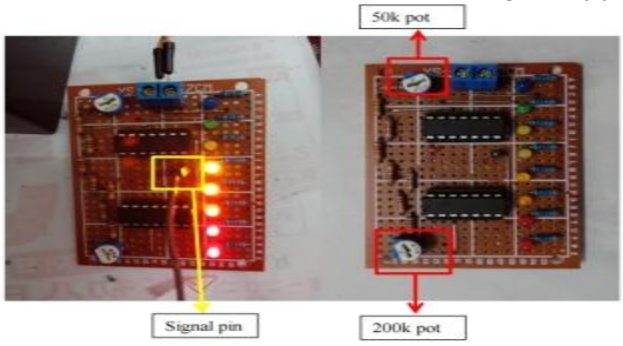

FIGURE 8(C). The completed voltage level indicator circuit.

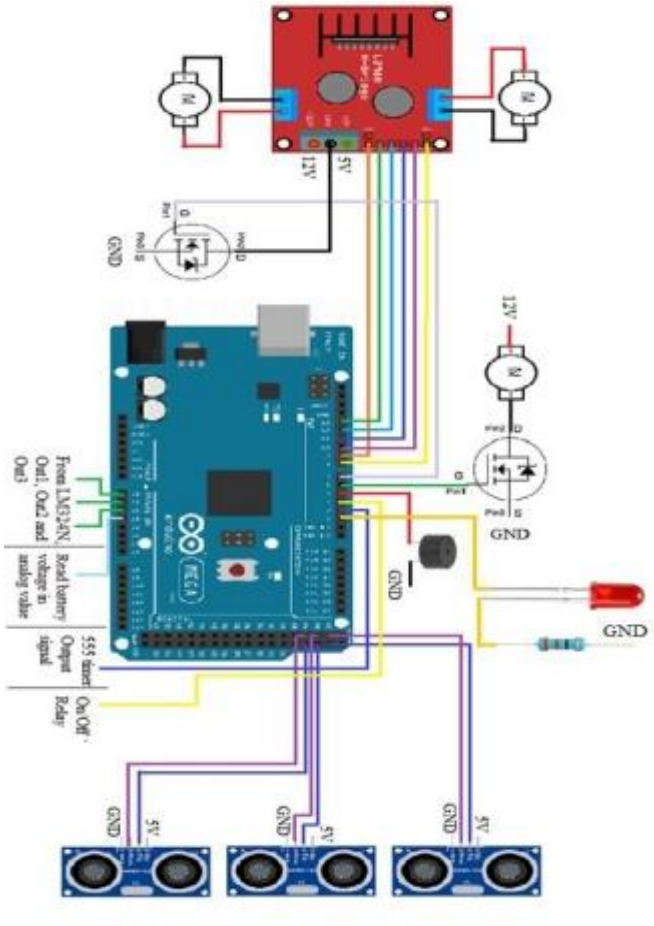

FIGURE 8(D). Full circuit connection.

D. Arduino IDE Programming

The Arduino IDE software is used to write the necessary code. The part of the code generated is shown in Figure 9(a). Section 1 includes the required libraries, such as wire.h, ultrasonic.h and 53L298N.h. In section 2, the values for variables IN1, IN2, IN3, IN4, ENA and ENB are assigned. Then section 3 is the declaration for three ultrasonic sensors and the L298N motor driver. Pin 23, 25 and 27 are the trigger pins and pin 22, 24 and 25 are the Echo pins for the ultrasonic sensor 1, 2 and 3. The pins ENA, IN1 and IN2 to motor1 (left dc motor) and ENB, IN3 and IN4 for motor2 (right dc motor). Section 4 declares the rest of the variables as type int.

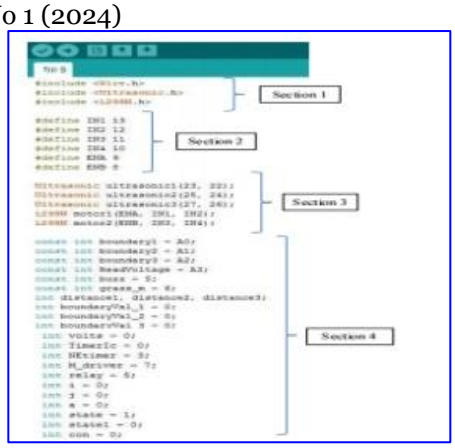

FIGURE 9(A). Part of the code generated.

In order for the device to be automated, the path must be well-designed. A S shape pattern is used in the algorithm of path design. To begin, the prototype is placed at the bottom left of the cutting area. The prototype then moves in an S pattern from one corner to the other until it reaches the border, as shown in Figure 9(b). This is an automated system when no obstacles or nothing approaches the prototype. To demonstrate this, the cutting area is set to 3m x 3m length and width. The boundary of the area is installed with a perimeter wire, the signal from the 555 timer is running through the wire. The prototype will start from the bottom left corner and move forward until it reaches the boundary. When the prototype reaches the boundary, the front inductor sensor will pick up the signal from the wire and know that it has reached the boundary, then the prototype will make a turn to the right and go forward for few steps, and then it will turn right and move forward again. The red line shows the path of the prototype needs to travel.

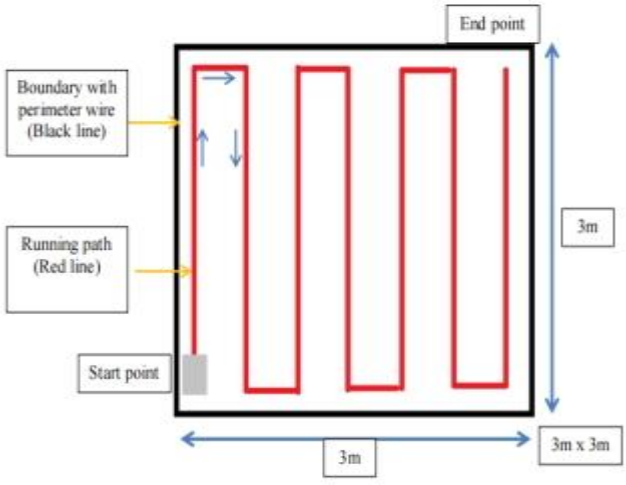

FIGURE 9(B). The path without the obstacles.

When the ultrasonic sensor detects an object, the prototype turns left, moves forward a short distance, then turns right, moves forward a few seconds, then turns right, moves forward till it reaches the original route, after which it returns to the forward direction, as shown in the Figure 9(c). During the trimming operation, when the battery voltage is detected is low, the prototype will automatically stop the trimming process and charge the battery. The automated system is primarily comprised of an inductor as the sensor that detects the boundary wire and the ultrasonic sensor that identifies objects or something approaches the prototype.

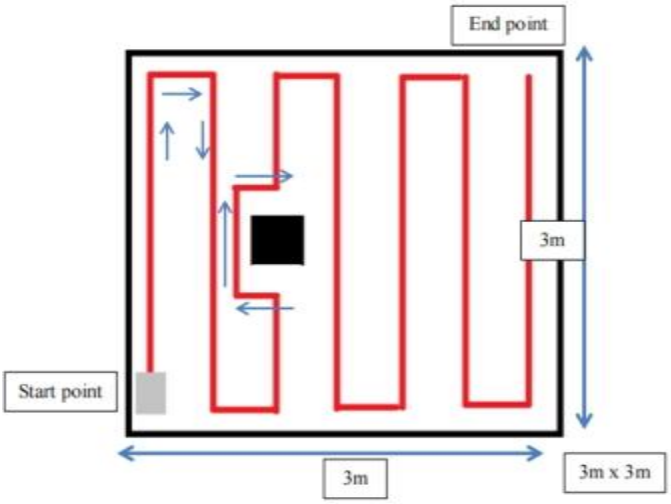

FIGURE 9(C). The path with the obstacles.

III. RESULTS AND DISCUSSION

The flowchart shown in Figure 9(d) describes the running process of the prototype. When the prototype is on, it will start its operation by activating the sensor. Then they measure the battery voltage condition to see whether the battery needs to be charged or not; If yes, the prototype stays idle, turns on the relay and charges the battery, if not, the prototype will start to move forward. The prototype will check whether the boundary is detected; if yes, it takes a U turn and moves to the new path, if no, the prototype will check for ultrasonic sensors. If an ultrasonic sensor detects something approaching the prototype, it will stop immediately, until the object moving away from the prototype. Then the prototype will check the front ultrasonic sensor to see if there is any obstacle; if yes, avoid the obstacle, if no, continue to move the prototype in a forward direction.

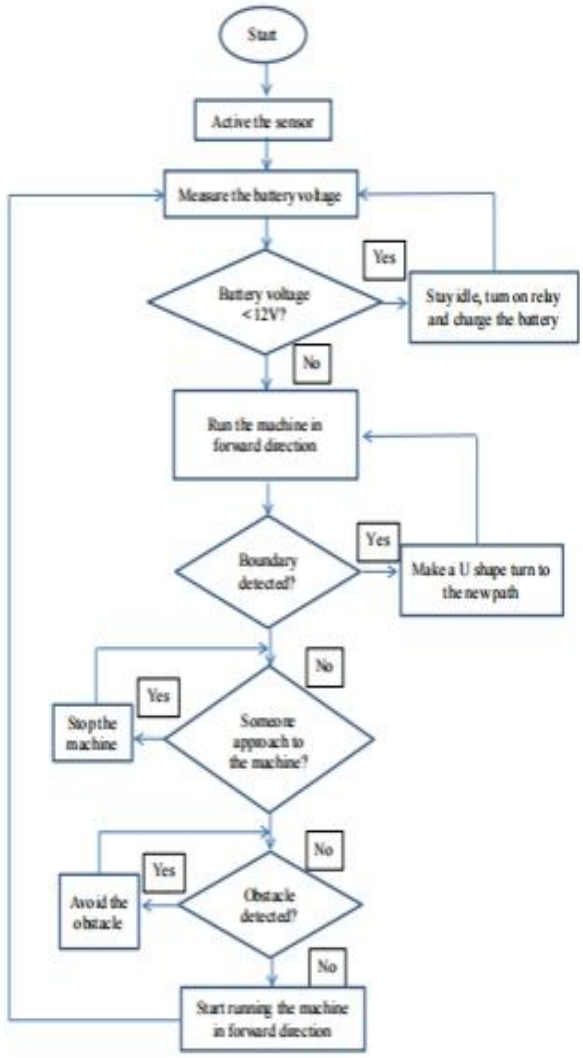

FIGURE 9(D). Flowchart of the algorithm.

Figure 9(e) and 9(f) show the top and side views of the completed automatic solar grass trimmer prototype. The top of the prototype has the solar panel to obtain the sunlight. The bottom of the prototype consists of boundary sensor and the grass trimming motor blade. The side view is the base of the prototype where the main components like microcontroller, motor driver, battery, charging circuit, ultrasonic sensors are placed.

(e) (f)

FIGURE 9(E). The top (e) and the front (f) view of the completed prototype.

Figure 10(a and b) shows the brackets, made out of galvanized wire, which are used to fix the perimeter wire in position. Since the testing for the trimming area is only 3m x 3m, four brackets are enough to fix at four corners. The perimeter wire is then passed through the bracket to form a square or rectangular trimming area as shown in Figure 10(c and d).

(a) (b)

FIGURE 10(A, B). The brackets for fixing the perimeter wire in place.

(c) (d)

FIGURE 10(C, D). The perimeter wire passing through the brackets.

Figure 10(e) shows the perimeter wire connected to the 555 timer signal generator circuit, the circuit is powered by the 12V power supply. Since there is no any external 12V power source, the power cable

extension is used with a 12V power adapter to convert the AC to DC.

FIGURE 10(E). The perimeter wire connected to the 555 timer signal generator.

A. Testing the Algorithm for Boundary Detection

In case of no obstacle detected by the front ultrasonic sensor, the prototype will move forward until it reaches the end of the boundary. When the perimeter wire is detected by the boundary sensor at the front, as shown in Figure 10(f), the prototype will turn 90° to the right and move forward for a few seconds. Then the prototype will turn right again to the new line. During the grass trimming process, if someone tries to approach the prototype, will cause the prototype to pause the process immediately to prevent any possible incident from happening.

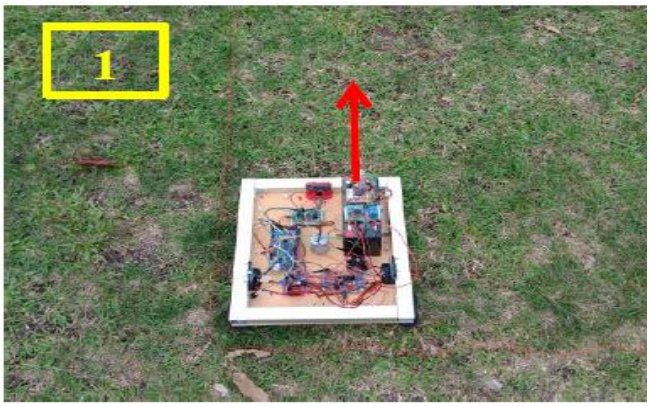

FIGURE 10(F). Boundary detection step 1.

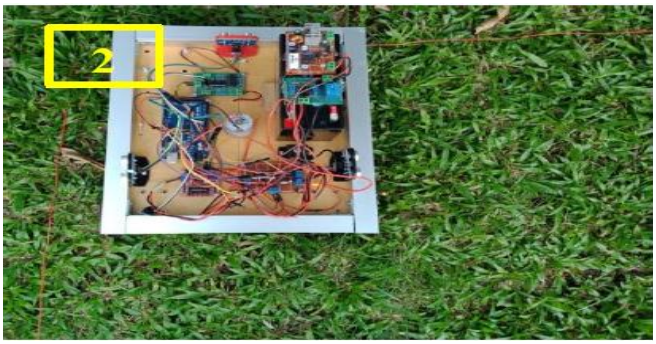

FIGURE10(F). Boundary detection step 2.

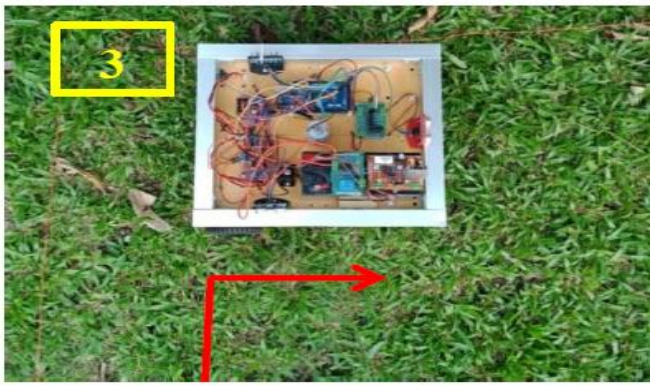

FIGURE 10(F). Boundary detection step 3.

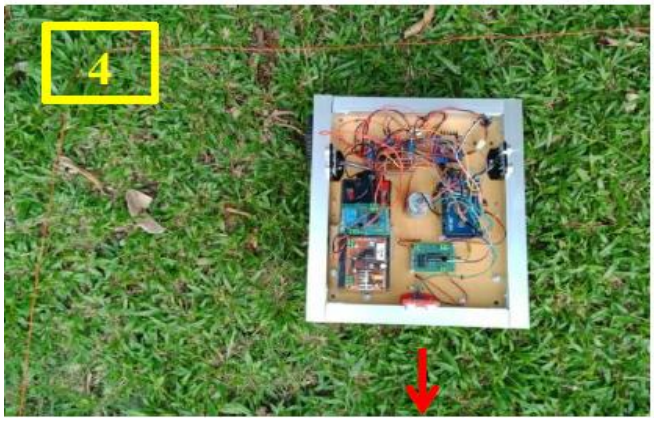

FIGURE10(F). Boundary detection step 4.

A similar test for boundary detection without any obstacles or human interference was conducted 5 times to see whether the result was the same or not and the results are shown in Table-1. The Boundary detection seems to be working fine all the time, because less actions need to be performed by the machine when it detects the boundary wire. Besides, the wire was placed right below of the boundary sensor and has been straighten, when the inductor distance between 2cm to 3cm to the wire, the analog value will increase to 450, therefore boundary detected. Then the machine will start to perform the actions. Although the machine might not be perfect when turn in 90 degrees and moving exactly in a straight line due to the lack of direction sensing, the algorithm is able to perform the actions required when certain condition is reached. During the second actions of boundary detection, the machine should turn in a reverse pattern compared to the first action. The following test was run continuously for 5 times boundary detection at once.

TABLE 1. Experiment for boundary detection.

Number of Test	Actions (Before boundary detection)	Boundary detected?	Actions (when boundary detected)

1	Move Forward	Yes	Turn right, move forward few steps. Turn right and move forward again
2	Move Forward	Yes	Turn right, move forward few steps. Turn right and move forward again
3	Move Forward	Yes	Turn right, move forward few steps. Turn right and move forward again
4	Move Forward	Yes	Turn right, move forward few steps. Turn right and move forward again
5	Move Forward	Yes	Turn right, move forward few steps. Turn right and move forward again

B. Testing the Algorithm for Obstacle Detection

The movement of the prototype when an obstacle is detected is shown in Figure 10(g). When the front ultrasonic sensor detects there is an obstacle (< 30cm to the front ultrasonic sensor), the prototype will turn to the left and move forward until the right ultrasonic sensor detects the prototype crosses the edge of the obstacle. Then the prototype will turn in the right direction for 90° and move forward again until it reaches another edge of the obstacle, as shown in step 3 and 4. The prototype will turn to the right 90° and move forward again until the right sensor detects the presence of the obstacle. Lastly, it will turn 90° to the left and back to its original path as shown in step 5 and 6 respectively.

FIGURE 10(G). Obstacle detection step 1.

FIGURE10(G). Obstacle detection step 2.

FIGURE10(G). Obstacle detection step 3.

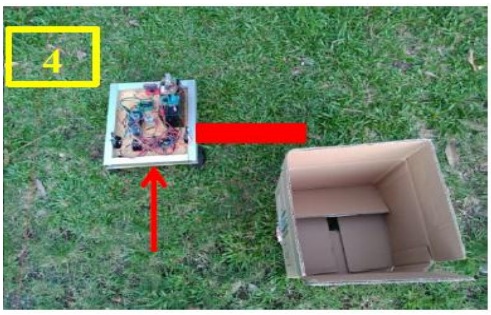

FIGURE 10(G). Obstacle detection step 4.

FIGURE 10(G). Obstacle detection step 5.

FIGURE 10(G). Obstacle detection step 6.

The similar test for obstacle avoidance was conducted 5 times to see whether the result was the same or not and the results are shown in Table-2. The experiment test result is not ideal and not as expected for each test performed. When several tests run in sequence, the machine starts to miss its original path, the offset increases when more tests is performed continuously. This is caused by the lack of direction sensing, the continuous testing leads to missing the original path of the machine. Even though the result is not better than any others, the machine is still performing the actions as expected when the front ultrasonic sensor detects an obstacle (distance < 30cm). Moreover, the ultrasonic sensor sometimes also receives some errors like the taller grass or the sensor itself. The lower positioning causes the front ultrasonic sensor detect the taller grass as an obstacle, or the sensor is not working normally, causes it to bump into the obstacle. The test was run continuously for 5 times obstacle detection at once.

TABLE2. Experiment for obstacle detection.

Number of Test	Actions (Before obstacle detection)	Obstacle detected?	Actions (when obstacle detected)
1	Move Forward	Yes	Turn left, move forward, then turn right, move forward again, then turn right, move forward until it reach the original path, then turn left and move forward again
2	Move Forward	Yes	Turn left, move forward, then turn right, move forward again, then turn right, move forward until it reach the original path, then turn left and move forward again
3	Move Forward	Yes	Turn left, move forward, then turn right, move forward again, then turn right, move forward until it reach the original path, then turn left and move forward again (some offset from the original path)
4	Move Forward	Yes	Turn left, move forward, then turn right, move forward again, then turn right, move forward and not reaching the original path, this is due to the lack of direction sensing, the continuous test causes the machine to miss its original path.
5	Move Forward	Yes	The machine bumps to the obstacle due to the error receives from the ultrasonic sensor. Therefore, the machine keeps moving forward and bump to the obstacle.

IV. CONCLUSION

The development and testing of an Arduino-based automated solar grass trimmer has been successfully completed. The voltage level indicator circuit design functions flawlessly, and the boundary detection circuit performs well. The implemented algorithm ensures effective operation, and field testing on a grass field confirms satisfactory performance. However, an observation reveals that the prototype faces challenges in moving in a straight line due to the limited number of sensors employed. To address this

issue, it is recommended to integrate either a compass sensor or a gyroscope sensor into the project. These sensors can accurately determine the machine's direction within a 0 to 360-degree range, allowing the machine to make necessary adjustments to maintain its original direction.

Furthermore, the current use of simple geared DC motors with a low RPM of 30 presents limitations. Unlike stepper motors, these DC motors lack feedback or pulse control for each step of movement. Consequently, one of the motors may rotate at a different speed than the others, leading to deviations in the machine's trajectory. To enhance precision, it is suggested to explore the use of stepper motors or implement feedback mechanisms for the existing DC motors in future iterations of the solar grass trimmer prototype.

ACKNOWLEDGEMENT

We thank the anonymous reviewers for the careful review of our manuscript.

FUNDING STATEMENT

This work does not have any funding support.

AUTHOR CONTRIBUTIONS

Thangavel Bhuvaneswari: Writing – Original Draft Preparation;

Venugopal Chitra: Writing – Review & Editing;

Sarah Immanuel: Writing – Review & Editing;

Emerson Raja: Writing – Review & Editing;

Chua Wei Chern: Writing – Review & Editing.

CONFLICT OF INTERESTS

No conflict of interests were disclosed.

ETHICS STATEMENTS

Our publication ethics follow The Committee of Publication Ethics (COPE) guideline. https://publicationethics.org/

REFERENCES

[1] T. B. Thangavel, C. VenuGopal, S. Immanuel, E. Raja, and W.C. Chua, "Design and Development of an Arduino Based Automated Solar Grass Trimmer," *IJORAS*, vol. 6, no. 1, pp. 46–58, 2024. DOI: https://doi.org/10.33093/ijoras.2024.6.1.7

[2] J.S. John, S.M. Dash, A. Sharma, A. Kashyap and V. Yadav, "Design and Analysis of Solar Powered Automated Lawn Mower with Vacuum Cleaner," in *2022 International Conference on Advances in Computing, Communication and Applied Informatics (ACCAI)*, pp. 1-5, 2022. DOI: https://doi.org/10.1109/ACCAI53970.2022.9752583

[3] M. Manimegalai, V. Mekala, N. Prabhuram and D. Suganthan, "Automatic Solar Powered Grass Cutter Incorporated with Alphabet Printing and Pesticide Sprayer," in *2018 International Conference on Intelligent Computing and Communication for Smart World (I2C2SW)*, Erode, pp. 268-271, 2018. DOI: https://doi.org/10.1109/I2C2SW45816.2018.8997301

[4] A. Basavaraju, E.S. Ram, N.R. Prasad, J.S. Kumar and M.V. Kumar, "Design and Development of Solar Based Grass Cutter Using IoT," *International Research Journal of Modernization in Engineering Technology and Science*, vol. 6, no. 2, 2024. DOI: https://doi.org/10.56726/IRJMETS49207

[5] S.P. Jagdale and P. Rajput, "Android Controlled Solar based Grass Cutter Robot," *International Journal of Engineering Research & Technology*, vol. 9, no. 7, pp. 750-753, 2020. DOI: https://doi.org/10.17577/ijertv9is070276

[6] M.O. Okwu, L.K. Tartibu, D.R. Enarevba, O.J. Oyejide, O.B. Otanocha and S. Adumene, "Development of a Light Weight Autonomous Lawn Mower and Performance Analysis using Fuzzy Logic Technique," in *2022 International Conference on Artificial Intelligence, Big Data, Computing and Data Communication Systems (icABCD)*, Durban, South Africa, 2022, pp. 1-9. DOI: https://doi.org/10.1109/icABCD54961.2022.9856342

[7] N.L. Puthra, S.K. R, Bhavan, M.T. M and V.S, "Design and Fabrication of Automatic Lawn Mower," *International Journal of Scientific Research in Mechanical and Materials Engineering*, vol. 8, no. 3, pp. 22-26, 2024. DOI: https://doi.org/10.32628/ijsrmme24834

[8] A.A. Okafor, E.C. Nwadike, A.E. Ilechukwu, and J.E. Dara, "Design and Fabrication of a Solar-Powered Lawn Mower for Health Facility Landscaping," *Medicine & Community Health Archives*, vol. 2, no. 05, pp. 179-188, 2024. DOI: https://doi.org/10.23958/mcha/vol02/i05/54

[9] N. Ramachandran, N. Kumar, S.K. Rajeshwaran, R. Jeyaseelan and S. Harrish, "Design and Fabrication of Semi-Automated Lawn Mower," *International Journal of Innovative Technology and Exploring Engineering*, vol. 8, no. 10, pp. 943-944, 2019. DOI: https://doi.org/10.35940/ijitee.J9092.0881019

[10] J. -C. Liao, S. -H. Chen, Z. -Y. Zhuang, B. -W. Wu and Y. -J. Chen, "Designing and Manufacturing of Automatic Robotic Lawn Mower," *Processes*, vol. 9, no. 2, 2021. DOI: https://doi.org/10.3390/pr9020358

[11] A.J. Farhan, "Fabrication and Development Low Cost Dual Axis Solar Tracking System," *IOP Conference Series: Materials Science and Engineering*, vol. 757, no. 1, pp. 012042, 2020. DOI: https://doi.org/10.1088/1757-899X/757/1/012042

[12] J.E. Okhaifoh and D.E. Okene, "Design and Implementation of a Microcontroller Based Dual Axis Solar Radiation Tracker," *Nigerian Journal of Technology*, vol. 35, no. 3, pp. 584–592, 2016. DOI: https://doi.org/10.4314/njt.v35i3.17

[13] E.M.H. Arif, J. Hossen, G.R. Murthy, T. Bhuvaneswari, P. Velrajkumar, and C. Venkataseshaiah, "A survey on neuro-fuzzy controllers for solar panel tracking systems," *Far East Journal of Electronics and Communications*, vol. 18, no. 7, pp. 981-1003, 2018. DOI: https://doi.org/10.17654/EC018070981

[14] G.R. Rajeshwar, C.A. Bhimrao, K.D. Sajjan, and R.K. Khandebharad, "Solar grass cutter using arduino uno," *International Journal of Advanced Research in Science, Communication and Technology*, vol. 3, issue 1, pp. 201-206, 2023. DOI: https://doi.org/10.48175/ijarsct-12031

[15] C. Palanisamy, "Smart manufacturing with smart technologies – a review," *International Journal on Robotics, Automation and Sciences*, vol. 5, no. 2, pp. 85–88, 2023. DOI: https://doi.org/10.33093/ijoras.2023.5.2.10

[16] V. P. Jawanjal, S. S. Nikam, P. P. Deshmane, A. R. Pawar, and A. R. Mahajan, "Design and Fabrication of Automatic Solar Grass Cutter," *International Journal of Advanced Research in Electrical, Electronics and Instrumentation Engineering*, vol. 6, no. 4, pp. 2648–2652, 2017, URL: https://www.ijareeie.com/upload/2017/april/37_Design.pdf (Accessed: 19 Feb, 2024).

[17] Y.S. Bong and G.C. Lee, "A contactless visitor access monitoring system," *International Journal on Robotics, Automation and Sciences*, vol. 3, pp. 33–41, 2021. DOI: https://doi.org/10.33093/ijoras.2021.3.6

[18] C.C. Lim, K.S. Sim, and C.K. Toa, "Development of visual-based rehabilitation using sensors for stroke patient," *International Journal on Robotics, Automation and Sciences*, vol. 2, pp. 25–30, 2020. DOI: https://doi.org/10.33093/ijoras.2020.2.4